Slow Released Nano-pesticide Platform Based on Metal Organic Framework for Delivery Avermectin, Cytotoxicity and Insecticidal Propertiesslow Released Nano-pesticide Platform Based on Metal Organic Framework for Delivery Avermectin, Cytotoxicity and Insecticidal Propertiesslow Released Nano-pesticide Platform Based on Metal Organic Framework for Delivery Avermectin, Cytotoxicity and Insecticidal Properties

Feng Gao
Tai'an Culaishan forest farm
Xiaoyu Xu
Shandong Agricultural University
Piao Dong
Shandong Agricultural University
Yixiao Qin
Shandong Agricultural University
Chenggang Zhou
Shandong Agricultural University
Luqin Qiao
Shandong Agricultural University
Huixiang Liu
Shandong Agricultural University
Zongtao Chang
Muping District forest resources protection monitoring service center
Yanxue Liu (liuyouyou2018@163.com)
Shandong Agricultural University https://orcid.org/0000-0002-1264-1441
Chenyu Su
Shandong Agricultural University

Research

Keywords: CuBTC, Avermectin, Nano-pesticide, Cytotoxicity, Bioassay

Posted Date: March 3rd, 2021

DOI: https://doi.org/10.21203/rs.3.rs-250879/v1

Abstract

Background: Pests affect the sustainable development of agriculture and forestry, and seriously threaten food safety and ecological health, the research for efficient and green control measures never stop. Pesticides are currently the most effective means to control pests and ensure food supplies. However, the various drawbacks of traditional pesticide formulations make the utilization low, and most of active ingredients flow into the air, groundwater and soil, destroying the environment. In this research, a novel nano pesticide formulation was synthesized to improve the utilization, with control release performance and anti-photolysis especially. CuBTC, a metal organic framework (MOF) material, was designed as carrier to absorb avermectin (AVM), a commonly used pesticide in agriculture and forestry, to prepare nano pesticide.

Results: The prepared AVM@CuBTC had slow release properties, could be released continuously for about 120 h, and the cumulative release exceed 91.5%, and had a more stable release process under different acid-base conditions. The particle size of AVM@CuBTC was about 450 nm, and the loading efficiency reached 38%. The AVM@CuBTC nano pesticide could protect AVM from photolysis, and the amount of degradation was reduced by 50.7% after 5 d treatment. In addition, the particles AVM@FITC@CuBTC were prepared by labeling with fluorescein isothiocyanate (FITC) to research the distribution on larval epidermis, to clarify the coverage, adhesion and permeability of AVM@CuBTC. Finally, the cytotoxicity and contact toxicity of AVM@CuBTC was compared with free AVM, the cytotoxicity and contact toxicity increased by 42.4% and 39.6%, respectively.

Conclusion: The cytotoxicity and contact toxicity of AVM are the key factors for the control of pests. Applying AVM@CuBTC to the prevention and control of agricultural and forestry pests is of great significance to the reduction of pesticides and environmental friendliness.

1. Introduction

At present, there are about 9,000 species of pests, and more than 50,000 species of plant pathogens seriously restrict the development of agriculture and forestry worldwide [1, 2]. They feed on plants, spread pathogenic microorganisms, and cause huge economic and ecological losses to agriculture and forestry [3]. Compared with other control measures, chemical control has the advantages of low cost and high adaptability, making it the main plant protection measure in agriculture and forestry [4, 5]. However, as humans pay more attention to the environment, the problem of traditional pesticide formulations becomes more and more acute [6]. The disadvantages of traditional pesticides such as poor dispersibility and retention make only 0.1% of pesticides are able to reach targets [7], not only the utilization rate is low, but also massive active ingredients flow into the environment, causing soil, groundwater and air pollution [8]. Therefore, there is an urgent need to develop an efficient solution to improve utilization and reduce pollution.

In recent years, nanotechnology has advanced by leaps and bounds, showing its advantages in many fields, especially environmental pollution remediation [9], microelectronics [10, 11], precision biology [12, 13]and so on. Researches have shown that as the particle size of pesticides decreases, the dispersibility in water [14], deposition of droplets on the leaves [15], the adhesion and penetration to pests are all improved [16]. These show that the application of nanotechnology in agriculture and forestry for the development of new pesticide formulations has great potential. It has been reported that various materials will be developed as delivery system for nano-pesticides. The tobacco mild green mosaic virus was self-assembled into soft material nanorods as a carrier for the nematicide crystal violet by Chariou [17]. Compared with free crystal violet, it has better soil mobility, in elution fractions of 25 to 50, the concentration was 3.6 times that of free crystal violet treatment. Li adopted the method of coordination assembly to prepare microcapsules to encapsulate pyraclostrobin, which reduced its toxicity to aquatic organisms by more than 6 times, so that pyraclostrobin, which is originally highly toxic to aquatic organisms, could be used in control of rice blast [18]. Liang had prepared a novel urease-responsive system for effective utilization of the herbicide and reducing environmental pollution [19]. The endimethalin was loaded in isocyanate-functionalized silica cross-linked with polyethylenimine to form a controlled release system with urease reaction characteristics, which can not only enhance the stability and light stability of endimethalin, but also can continue to control weeds for more than 50 days [20]. However, the high cost and cumbersome production process have always restricted the development of nano-pesticides, so it is necessary to develop a low-cost, simple production process nano-pesticide.

Metal organic framework (MOF) is a crystalline porous material with network structure formed by self-assembly of metal ions and organic ligands [21-24]. Its advantages such as high porosity, large specific surface area, regular pores, adjustable pore size have made it a research focus in the past decade [25, 26]. In addition to applications in gas storage [27], separation [28], catalysis [29], the high loading efficiency, stability and good slow-release performance of MOF have made it also perform well in drug loading. CuBTC was also known as HKUST-1, BTC=1,3,5-benzenetricarboxylate, CuBTC may be used as a pesticide delivery system due to its simple production process, low cost and large output [30, 31]. Avermectin (AVM) is a broad-spectrum and high-efficiency pesticide, which has the effect of bactericidal, insecticidal and nematicidal, widely used in the prevention and control of pests and diseases in agriculture and forestry [32]. However, the extremely poor water solubility, only 7.8 μg/L, and short half-life, less than 12 h in surface of soil or leaves, has severely limited the utilization rate of AVM [33]. Therefore, CuBTC was used as carrier to adsorb AVM to prepare nano-pesticides, which may improve the dispersibility and stability of AVM and ultimately effectively increase the utilization rate.

In this study, a nano-pesticide delivery system that could effectively improve the utilization of pesticides was designed, CuBTC was chosen as a carrier and absorbed AVM to prepare a nano-pesticide with high loading efficiency, slow release performance and high stability, for controlling pests and disease diseases in agriculture and forestry. The preparation of CuBTC adopted coordination control at room temperature, then the CuBTC powder was dispersed in the organic solvent dissolved with AVM, and AVM was fully adsorbed by CuBTC, and the nano pesticicde AVM@CuBTC was successfully prepared (Fig. 1). The structure of AVM@CuBTC were observed by scanning electron microscopy (SEM), the loading efficiency

was measured in different AVM concentration, and then the characterization of CuBTC was examined by dynamic light scattering (DLS), X-ray diffraction (XRD), thermogravimetric analysis (TGA), and specific surface area and pore size distribution analysis (BET). The release performance and stability of AVM@CuBTC at different temperatures and pHs was further measured. To further explore the application of AVM@CuBTC to pests, the common coleopteran pest *Monochamus alternatus* was selected as the research object [34, 35]. By utilizing the fluorescent staining technique, fluorescein isothiocyanate (FITC) was labeled with CuBTC to synthesize fluorescent AVM@FITC@CuBTC to research the distribution of AVM@CuBTC on the larval body surface, and the cytotoxicity of CuBTC and AVM@CuBTC in vitro were also investigated, finally at the individual level, the toxicity of AVM@CuBTC was determined and compared with free AVM.

2. Materials And Methods

2.1 Materials

The model pesticide, avermectin (AVM) (97%), was supplied by Aladdin Industrial Corporation (Shanghai, China). The AVM emulsifiable concentrates (EC) (5%) were provided by Shenzhen Noposion International Investment Co., Ltd. (Shenzhen, China). The copper nitrate trihydrate (99%), polyvinylpyrrolidone (PVP) and trimesic acid were purchased from Shanghai Macklin Biochemical Co., Ltd. (Shanghai, China). Methanol (analytical grade) was provided by Kermel Chemical Reagent Co., Ltd. (Tianjin, China). The 1×PBS (pH 7.2-7.4, 0.01 M) buffer, the conjugation-grade (purity>95%) fluorescein isothiocyanate (FITC), and trypan blue were provided by Coolaber Science & Technology Co., Ltd. (Beijing, China).

2.2 Preparation of AVM@CuBTC

2.2.1 Synthesis of CuBTC. According to the previously described approach, CuBTC were synthesized with minor modifications [36]. Copper nitrate trihydrate (900 mg) and PVP (200 mg) were dissolved in methanol (200 mL) uniformly under ultrasonic vibration, and trimesic acid (430 mg) were dissolved in methanol (150 mL). The trimesic acid methanol solution was dropped into metal salt solution with stirring (800 rpm) and reaction for 30 minutes. After standing 24 hours, the complex was centrifuged for 5 minutes (8000 rpm), the supernatant was discarded, a small amount of methanol was added to the precipitate, ultrasonically dispersed and then centrifuged, CuBTC was got after repeating five times.

2.2.2 Synthesis of AVM@CuBTC. The powder of CuBTC (30 mg) was dispersed in methanol, and the AVM (20 mg) was dissolved in methanol. The AVM methanol solution was added into CuBTC solution. The mixed solution was stirred (300 rpm) for 48 hours. The product was centrifuged for 5 minutes (8000 rpm) to remove unadsorbed AVM.

2.2.3 Synthesis of AVM@FITC@CuBTC. The method of synthesis of AVM@FITC@CuBTC was according to pervious research with modification [37]. FITC (1 mg) was dissolved in 10 mL absolute ethyl alcohol, and the powder of AVM@CuBTC (25 mg) was added into the solution. The solution was stirred (300 rpm) under dark condition for 4 hours, then the product was centrifuged for 5 minutes (8000 rpm), the

precipitate was dispersed in absolute ethyl alcohol, the AVM@FITC@CuBTC was gotten by centrifuging again.

2.3 Characterization

The morphology and structure of AVM@CuBTC was observed by scanning electron microscopy (SEM, Hitachi S-3400N, Japan). The size distribution of AVM@CuBTC was measured by a laser particle size analyzer (Nanobrook 90Plus PALS, USA). Powder X-ray diffraction measurements were carried out using an X-Ray diffractometer (SmartLab Ultima IV, Japan), and the resulting data was plotted in Origin. Thermogravimetric analysis (TGA) of CuBTC was performed with a thermal analyzer (Netzsch Q600, Germany) analyzer from 40 to 800 ℃ with a heat rate of 10 ℃/min. The pore size and specific surface area of CuBTC were determined by specific surface area and pore size distribution analyzer (Beishide 3H-2000, China).

2.4 Loading efficiency of CuBTC

Quantified CuBTC powder was taken accurately, excess methanol was added and ultrasonic dispersion uniformly. The model pesticide AVM was dissolved in methanol (75 mL) to prepare different concertation of AVM methanol solution. The AVM methanol solution was mixed with CuBTC solution, the mixed solution was stirred at 300 rpm for 48 hours. Finally, the mixed solution was centrifuged at 8000 rpm for 5 minutes, and the supernatant was taken to determine the free AVM content. The AVM content was analyzed by measuring the absorbance by using UV spectrophotometer (Shimadu UV-2450PV, Japan). The loading efficiency of CuBTC was calculated according to the following equation [38]:

$$\text{Loading efficiency of CuBTC (\%)} = \left(\frac{\text{Weight of total AVM-Weight of Free AVM}}{\text{AVM@CuBTC}}\right) \times 100$$

2.5 Stability test.

The samples were stored for 45 days at 15 ℃, 25 ℃, and 35 ℃, and samples were taken at regular intervals to determine the particle size and Zeta potential. And the powder of AVM@CuBTC were dispersed in 10 mL of water, then the treatment was spread on a 9.0 cm diameter culture dish and dried in dark at indoor temperature, Then the dishes were exposed to UV light. The retention of AVM in culture dish was entirely extracted by 20 mL methanol at different intervals and analyzing by UV spectrophotometer. AVM, AVM@EC were designed as controls under same conditions [39].

2.6 Controlled release of AVM@CuBTC

The release process of AVM@CuBTC was assayed using a modification of the research described by Guo [40]. The powder of AVM@CuBTC was weighed and dispersed in PBS and transferred into a dialysis bag. The dialysis was put into the release medium (500 mL of the methanol-PBS mixture, 20:80, v/v), which was used to dissolve the released AVM. The system of release was incubated in a shaker with an oscillation rate of 150 rpm. The mixture outside the dialysis bag was taken at different point, the release

process was analyzing the concentration of released AVM using UV spectrophotometer, finally equal volume of fresh release medium was added into the system. Simultaneously, the release processes of AVM@EC and AVM@CuBTC in different temperature and pH were performed as controls.

2.7 Distribution of AVM@CuBTC on larval surface

Firstly, AVM@CuBTC and AVM@FITC@CuBTC were dispersed in water, the filter paper was wetted with the solution. Then the well-developed larvae were picked and placed in the filter paper. After crawling to make the larvae fully contact with AVM@CuBTC or AVM@FITC@CuBTC. The distribution of AVM@CuBTC on the surface was observed by super depth-of-field 3D microscope, similarly the distribution of AVM@FITC@CuBTC was observed by a fluorescent stereomicroscope.

2.8 In vitro cytotoxicity of AVM@CuBTC

Trypan blue (4 g) was placed in beaker, small amount of distilled water was added to grind, transferred this solution to a 100 mL volumetric flask, diluted with distilled water to volume. Then the solution was filtered with filter paper and stored at 4 ℃, diluted to 0.4% when used. In an aseptic bench, the larvae were soaked in 70% ethanol for 20 minutes. The ethanol on the surface was absorbed to dryness by a sterile absorbent paper. Then the pronotum of larva was plunged by an insect needle, the blood cells were taken out by a dot capillary and diluted appropriately with PBS (10^7 cells/mL). After equal volume and different concentration of AVM@CuBTC solutions were added for a period of time, mixed the cell suspension with 0.4% trypan blue solution at a ratio of 9:1. Within three minutes, the live and dead cells were observed by a microscope and counted separately with a hemocytometer.

2.9 Bioactivity

The bioactivity of AVM@CuBTC against *Monochamus alternatus* assayed using a modification of the drug membrane contact method [41]. The powder of AVM@CuBTC were dispersed in water and diluted to concentration gradients (80, 40, 20, 10, 5 μg/mL), similarly, the filter papers were treated by the AVM@CuBTC solution, respectively. Thirty well-developed larvae were placed in a filter paper and crawled to make the larvae fully contact with AVM@CuBTC. The larvae treated with AVM@CuBTC were cultured in a 6 cm^3 breeding box with artificial feed. After 24 or 48 hours of cultivation, the survival of the larvae was investigated, and the larvae were considered dead if they were unable to move when touched with a brush.

2.10 Statistical analysis

All experiments in this work were repeated three times, and statistical analysis of the data was performed by analysis of varoamce (ANOVA) using DPS v 7.05. All graphical data are reported as the mean ± standard deviation (SD). Significance levels were set at * $p < 0.05$.

3. Results And Discussion

3.1 Characterization of AVM@CuBTC

In this study, the preparation of CuBTC adopted coordination control at room temperature, the final product AVM@CuBTC was light blue powder. As we could see, the powder of AVM@CuBTC and AVM@FITC@CuBTC could be dispersed in water evenly, and the AVM@CuBTC aqueous solution was light blue (Fig. 2A), AVM@FITC@CuBTC aqueous solution was blue-green (Fig. 2B). Fig. 2C was the XRD data of CuBTC and AVM@CuBTC, compared the simulation data of HKUST-1, there were diffraction peaks in 5.82, 6.72, 9.52, 11.16, 11.65, 13.47, 14.68, 15.09, 16.53, 17.53, 19.04, 20.27, 21.38, 23.46, 24.20, 26.05, 27.80, 28.85, 29.41, 30.42, 31.00, 31.95, 34.83, 35.32, 37.96, 39.24, 39.40, 40.48, 41.63, 42.84, 46.23, 46.89, 47.31, and the characteristic peak of CuBTC was consistent with the simulated data of HKUST-1, and the intensity was similar, indicating that the purity and crystallinity of the obtained sample were close to the simulated value. There was no significant difference in atlas between before and after loading, indicating that the loading process had no effect on the shape of the carrier. The type I Langmuir adsorption isotherm of CuBTC was shown in Fig. 2D, the CuBTC sample prepared in this study had a specific epidermis area of 139.99 m^2/g and a mesoporous pore size (Fig. 2E). There were open unsaturated Cu metal sites in CuBTC, so the catalytic and adsorption properties were excellent. Observing the thermogravimetric curve between 0-800 ℃ (Fig. 2F), it could be seen that the mass loss of the sample was 19% between 20-194.8 ℃, and the lost mass could correspond to solvent molecules or other guest molecules. A gentle curve appears after 194.8 ℃, this indicated that the sample remains stable until 263.9 ℃, and after 263.9 ℃, obvious mass loss started, indicating that the internal structure collapsed. Finally, at 348.4, the decline of the curve tended to be gentle, with a total mass loss of 64.1%, it showed that the CuBTC prepared in this study had good thermal stability.

In Fig. 3, the SEM images of the final products was displayed to research the structure of AVM@CuBTC. As we could see, the structure of the nano-particles was a regular and consistent octahedron, no other structural by-products were formed in the field of view, the particles were evenly dispersed, and were independent of each other, there was no adhesion. The particle size AVM@CuBTC was about 450 nm in images.

The calibration curve of AVM in methanol was linear in the concentration range of 5-50 μg/mL, and the regression equation was y=0.0182 x, the correlation coefficient was 0.9996 (Fig. 4A). Then the particle size of AVM@CuBTC was measured by DLS, as shown in the Fig. 4B, the average particle size was at 470 nm, and showing a single peak, indicating that the particle size distribution of AVM@CuBTC was concentrated, and no other by-products were formed. In order to determine the loading efficiency of AVM@CuBTC, 50 mg of CuBTC powder was dispersed in 75 mL of AVM methanol solution with different concentrations, respectively. Fig. 4C was drawn according to the relationship between loading efficiency and AVM concentration. It could be seen that as the concentration of the AVM methanol solution increases, the loading efficiency gradually increases, there was a maximum loading efficiency at 600 μg/mL, and the maximum loading efficiency was about 38%. After that, the loading efficiency no longer increases with the AVM concentration. The above results proved that as a pesticide carrier, CuBTC has a stable structure, uniform particle size, and ideal drug loading. It is a potential nano-pesticide Carrier.

3.2 Stability of AVM@CuBTC

In order to verify the stability of AVM@CuBTC, the powder of AVM@CuBTC were placed at different temperatures, and the particle size and Zeta potential were measured regularly. It could be seen that the particle size (Fig. 5A) and Zeta potential (Fig. 5B) remained basically unchanged at different temperatures, which indicated that AVM@CuBTC could be stable within a certain temperature range. As introduced in the previous article, the half-life of AVM was short, the characteristic structure of the conjugated double bond and the 16-membered ring macrolide structure made it easy to degrade under light [42]. Therefore, the retention of AVM after treatment was measured to clarify the protective effect of AVM@CuBTC (Fig. 5C). By comparison, it could be seen that under the condition of ultraviolet light irradiation, with the extension of the treatment time, the retention rate of each treatment group decreased. After 72 hours, the retention rate of the F-AVM treatment group was less than 5%, and the AVM@EC treatment group was only about 15%. On the contrary, the retention rate of the AVM@CuBTC treatment group was still more than 50% after 120 h. This may be because AVM@CuBTC gradually released AVM after treatment, and the released AVM was degraded, resulting in a decrease in retention rate, which indicated that CuBTC could effectively protect AVM from photolysis. In addition, it could be seen that AVM@CuBTC has a more stable performance in acid-base system, and the retention rate after 120 h were 62.2% and 69.4% in pH 5.0 and pH 9.0, respectively. This may be due to the increased interaction between CuBTC and AVM under acid-base conditions, and the interaction made the protective effect further enhanced. Under dark condition (Fig. 5D), it could be seen that the retention rate of the five treatment groups exceeded 70%. The retention rate of the AVM@CuBTC treatment group (85%) was significantly higher than the F-AVM treatment group (71%) and the AVM@EC treatment group (73%), which was consistent with the results under light conditions. Under different pH conditions, the pH 9.0 group still had the highest retention rate, which was close to 90%. The unique porous structure of CuBTC itself was the key to protecting AVM from ultraviolet light. The photodegradable nature of AVM limited the application and caused waste of active ingredients in production, and AVM@CuBTC could effectively protect AVM from photodegradation, compared with the F-AVM treatment group, the amount of degradation was reduced by 50.7%. Not only the properties were stable, but also could effectively protect the active ingredients, therefore the AVM@CuBTC was a qualified nano-pesticide carrier.

3.3 Controlled release of AVM@CuBTC

The frequency of pesticide application could be effectively reduced by extending the release period, so that the environmental pollution, pesticide abuse and other problems could be controlled [43]. The release performance of AVM@CuBTC was studied under different temperature and pH gradients to simulate the release in natural environment. The temperature and pH selected in this study represented the common environmental temperature and pH range during pesticide application. Firstly, the release performance of AVM@CuBTC and AVM@EC was compared, At the condition of 25 °C and pH 7.0, the release process of AVM@CuBTC was stable without burst release, and the release process lasted for 72 h, the cumulative release amount reached 91.5%. On the contrary, the cumulative release amount of AVM@EC treatment group released 88% within 6 h, and the burst release was obvious (Fig. 6A). These results showed that,

compared with the commercially formulations, the release performance was better, longer sustained release time, and higher cumulative release amount. To achieved the desired control effect in agriculture and forestry, the pesticides were often overused due to the short release duration, this increased production costs and exacerbated the problem of residues and drug resistance, hence the development of AVM@CuBTC would provide solutions for it. Next, the release of AVM@CuBTC under different temperature conditions were explored (Fig. 6B). At 15℃, 25℃ and 35℃, the release process of AVM@CuBTC were still stable, with cumulative release exceeding 96 h, and the cumulative release were close to 90%. With the increase of temperature, the release rate of AVM gradually increased, the release rate under 15℃ was slower than that 25℃, under 35℃, the release rate was the fastest and the cumulative release amount was the highest, reaching 91.4%. The increase in temperature accelerated the release of AVM, but has little effect on cumulative release amount. On the other hand, AVM@CuBTC could still be released stably at different pH conditions, the release rate was the fastest at pH 7.0 and the cumulative release amount was the largest, followed by pH 5.0, the cumulative release amount decreased significantly, about 83.5%, while the lowest was pH 9.0 treatment group, the cumulative release amount was only 79.2%, even less than 80% (Fig. 6C).

The acid-base environment may increase the unsaturated metal sites in CuBTC, thereby enhancing the interaction between CuBTC and AVM, making the binding stronger, or the released AVM was re-adsorbed, thus prolonging the release period and reducing the cumulative release amount. These above results indicated that AVM@CuBTC showed well slow-release performance within regular temperature and pH range with stable release, and no sudden release. The further development of AVM@CuBTC into pesticide formulations is of great significance for pesticide reduction and environmentally friendly agriculture.

3.4 Distribution on larval epidermis

Contact toxicity (pesticides enter the pest body through the epidermis after contact to exert its activity), which is limited by the dispersibility of traditional preparations [8]. The poor coverage adhesion and permeability of active ingredient on the larval epidermis, is an important factor of restricting the contact toxicity, so the ultra-depth-of-field microscope, SEM and fluorescence microscopy was used in this study to observe the distribution of AVM@CuBTC, and the figures were listed.

Firstly, the distribution of AVM@CuBTC on the epidermis of the larva was observed under ultra-depth-of-field microscope (Fig. 7), it could be seen that the larval epidermis showed blue overall. The AVM@CuBTC did not fall off and still adhered to the larval epidermis after crawled for a period of time, because of the better coverage and adhesion. The powder of AVM@CuBTC were dispersed in water，then the larvae were observed by scanning electron microscope after treated by AVM@CuBTC solution. According to the SEM image (Fig. 8), it could be seen that the particle of AVM@CuBTC could still maintain a complete structure on the epidermis of the larvae, with a relatively dispersed distribution. Most of AVM@CuBTC particle were distributed on the folds of the epidermal structure, in addition, more AVM@CuBTC particle were distributed around the valve and the roots of the chaeta, and these two parts may be important passway of particle into the larval body.

Next, the larva was treated with fluorescent AVM@FITC@CuBTC for some time now, and observed under fluorescence microscope. As is shown in Fig. 9, there was obvious uniform green fluorescence on larval epidermis, which also verified the coverage and adhesion of AVM@FITC@CuBTC on epidermis. In addition to the fluorescence observed on epidermis, there was also a fluorescence distribution in larval body, which indicated that AVM@FITC@CuBTC had successfully penetrated into larval body through the epidermal tissue, this showed that the good permeability of AVM@FITC@CuBTC. At the same time, there are multiple bright fluorescent particles distributed beside the valve on both sides of the larva. The particle size of AVM@FITC@CuBTC was much smaller than the diameter of the valve, and the particles could easily pass through the valve and enter into the larval body, so the valve may be an important pass way for nano pesticide enter the larval body.

Compared with traditional pesticide formulations, the smaller particle size, larger specific surface area, and higher water dispersibility of nano pesticides make the better coverage, adhesion and permeability. Because the nano formulation significantly improved the diffusion and permeability of pesticides, and the efficiency of the active ingredients entering into the larval body had also been increased, finally, the insecticidal activity was enhanced. The AVM@CuBTC nano-pesticide prepared in this study had high coverage, good adhesion and permeability on larval epidermis, and it may have a good effect on enhancing the contact toxicity of pesticides, and achieved the ideal control effect with smaller consumption, thereby reducing the abuse of pesticides.

3.5 In vitro cytotoxicity of AVM@CuBTC

In the research of medical drug delivery, well targeting, biocompatibility, and stability are usually all needed for nano drug delivery systems, at the same time, the safety of the carrier and the cellular uptake are also the focus of research. Therefore, in this study, we explored the effect of CuBTC and AVM@CuBTC on cytotoxicity in Vitro (Fig. 10A), it could be concluded that CuBTC has a little toxicity to insect blood cells, and the toxicity was much lower than that of AVM. When the concentration was 16 μg/mL, the corrected mortality of CuBTC on insect blood cells was only 18%, which was only one-fifth of the F-AVM treatment group at the same concentration. Obviously, the cytotoxicity of the AVM@CuBTC treatment group was higher than that of the AVM@EC treatment group and the F-AVM treatment group at all concentrations, especially in the low concentration. For example, The mortality rate of AVM@CuBTC was 13.9% at 1 μg/mL, while the F-AVM treatment group was only 6.19%, which was more than double that of the F-AVM treatment group, indicating that AVM@CuBTC had a greater increase in cytotoxicity at low concentrations, and this part of the increase in toxicity was not caused by the cytotoxicity of CuBTC. Therefore, we speculated that CuBTC, as a carrier, significantly enhanced cellular uptake of AVM under low-concentration conditions, resulting in an increase in cell mortality. Although the cell mortality of AVM@CuBTC was still higher than the other two treatments and was not significant after the concentration was increased, it may be because the high concentration of AVM makes up for the low cellular uptake. In addition, we have also done the effects of different temperatures on cell mortality (Fig.

10B), as the temperature increased, the cell mortality in each treatment group gradually increased. The highest mortality still was the AVM@CuBTC treatment group at the same temperature. Compared with F-AVM and AVM@EC, there was a greater impact on cell mortality in the AVM@CuBTC treatment group by the increase in temperature. Based on this, we speculated that this may be due to the way blood cells take in AVM@CuBTC through endocytosis, increase of cell activity leaded to improved cellular uptake and mortality with the temperature. And then, the effect of different treatment times on cell mortality was researched (Fig. 10C), and it could be concluded that with the extension of the treatment time, the cell mortality of each treatment group gradually increased, the mortality of AVM@CuBTC (60.6%) was higher than F-AVM (39.7%) and AVM@EC (44.8%) after 8 h treatment. Results were consistent with temperature variables, the effect of treatment time on mortality was also the most obvious in the AVM@CuBTC group. In summary, insect blood cells took up AVM@CuBTC through endocytosis, and AVM@CuBTC could significantly improve the cytotoxicity of AVM by increasing the cellular uptake.

3.6 Contact toxicity of AVM@CuBTC

Finally, the third instar larva of *Monochamus alternatus* was used as the research object to verify the effect of AVM@CuBTC on contact toxicity at the individual level. It could be seen that CuBTC has low contact toxicity to larvae, as the concentration increases, the corrected mortality of larvae never exceeds 10%, indicating that the carrier itself is harmless to the target organism and is an environmentally safe pesticide carrier. Among the three treatment groups, AVM@CuBTC had the highest lethality to larvae (Fig. 11). At 24 h, the corrected mortality rates were 8.9%, 22.2%, 40.0%, 52.2% and 66.7%, respectively, at 48 h, the corrected mortality rates were 13.3%, 28.9%, 48.9%, 63.3% and 87.8%, respectively, which were higher than those of the F-AVM treatment group of 7.8%, 18.9%, 34.4%, 54.4% and 76.7%. The lethality rate of AVM@CuBTC increased by 70.5% at low concentrations (5 μg/mL), however the contact toxicity increased by only 14.5% at high concentrations (80 μg/mL). In general, AVM was adsorbed CuBTC to prepare AVM@CuBTC nano pesticide could effectively improve the contact toxicity of active ingredients to target organisms, which also confirmed the results of the previous parts of research. Because the better coverage, adhesion, permeability, higher cellular uptake and cytotoxicity of AVM@CuBTC, these factors worked together to make the contact toxicity level higher than that of traditional pesticide formulations at the individual, so there were broad application prospects in the application of AVM@CuBTC to agriculture and forestry for pest control.

4. Conclusions

In this study, an original nano pesticide AVM@CuBTC was prepared, which was used MOF material CuBTC as carrier to adsorb AVM. The AVM@CuBTC was with a particle size of approximately 450 nm and a loading efficiency 38%, and prevented AVM from degradation, the amount of degradation was reduced by 50.7%. The AVM@CuBTC could release AVM stably over 4 d, and the amount of cumulative release reached 90%, and the release period was longer in acid-base environment, the amount of cumulative release was reduced, but it also exceeded 80%. The distribution of AVM@CuBTC were observed by labeling with FITC, and the observation results showed that AVM@CuBTC had a wide distribution on the

larval epidermis, strong adhesive and good penetrability, could carry active ingredients efficiently penetrate the larval epidermis and enter larval body. Then, the cytotoxicity of CuBTC and AVM@CuBTC to insect blood cells was investigated in vitro, CuBTC has low toxicity to blood cells, but it could significantly increase the cytotoxicity of AVM. Finally, the contact toxicity of AVM@CuBTC to the 3rd instar larvae of *Monochamus alternatus* was determined at the individual level, the preparation of AVM@CuBTC nano pesticide by using CuBTC to adsorb AVM could effectively improve the contact toxicity of AVM to 3rd instar larva, and the contact toxicity increased by 39.6%. In summary, the AVM@CuBTC was applied to pest control in agriculture and forestry with broad prospects.

Declarations

Acknowledgements

The authors acknowledge the following people for their contributions: Shanshan Liu, Tao Chen.

Authors' contributions

GF, YX and CG contributed to conception. ZT, HX, LQ contributed to study design. DP and YX contributed to data acquisition. CY and XY contributed to original writing. YX, CG a contributed to review and editing. All authors read and approved the final manuscript.

Funding

This study was supported by the Shandong Agricultural Science and Technology Innovation (Forestry Science and Technology Innovation) Project (2019LY003).

Availability of data and materials

All data generated or analyzed during this are included in this published article.

Ethics approval and consent to participate

Not applicable.

Consent for publication

Not applicable.

Competing interests

All authors declare that they have no competing interests.

Author details

[1] *Tai'an Culaishan forest farm, Tai'an, Shandong 271027, P. R. China;*

[2] College of plant protection, Shandong agricultural university, Tai'an, Shandong 271018, P. R. China;

[3] Shandong research center for forestry harmful biological control engineering and technology, Shandong agricultural university, Tai'an, Shandong 271018, P. R. China;

[4] Muping district forest resources protection monitoring service center, Yantai□Shandong 264001, P. R. China;

[5] College of animal and veterinary medicine, Shandong agricultural university, Tai'an, Shandong 271018, P. R. China.

References

1. Yusoff SNM, Kamari A, Aljafree NFA. A review of materials used as carrier agents in pesticide formulations. Int J Environ Sci Te. 2016;13:1–18. DOI:10.1007/s13762-016-1096-y.
2. Lorena P, Gudeta WS, Sofia G, Riikka K, Edmundo B, Mary NM, Charles M, Mattias J. Effects of agroforestry on pest, disease and weed control: A meta-analysis. Basic Appl Ecol. 2015;16:573–82. DOI:10.1016/j.baae.2015.08.006.
3. Kobayashi F, Yamane A, keda T. The Japanese pine sawyer beetle as the vector of pine wilt disease. Annu Rev Entomol. 1984;29:115–35. DOI:10.1146/annurev.en.29.010184.000555.
4. Guedes RNC, Smagghe G, Stark JD, Desneux N, pesticide-induced stress in arthropod oests for optimized integrated pest management programs, Annu Rev Entomol. 61 (2016) annurev-ento-010715-023646. DOI:10.1146/annurev-ento-010715-023646.
5. Mckee SC, Shwiff SA, Anderson AM. Estimation of wildlife damage from federal crop insurance data. Pest Manag Sci. 2020. DOI:10.1002/ps.6031.
6. Brooks GT. Pest management science (formerly pesticide science), Pest Manag Sci 56 (2000). DOI: (SICI)1526-4998(200001)56:13.0.CO,2-8.
7. Enserink M, Hines PJ, Vignieri SN, Wigginton NS, Yeston JS. Smarter pest control. The pesticide paradox. Introduction Science. 2013;341:728–9. DOI:10.1126/science.341.6147.728.
8. Bonmatin JM. Stop poisoning farmands. Nature. 2015;521:59. DOI:10.1038/521S57a.
9. Massinon M, De Cock N, Forster WA, Nairn JJ, Mccue SW, Zabkiewicz JA, Lebeau F. Spray droplet impaction outcomes for different plant species and spray formulations. Crop Prot. 2017;99:65–75. DOI:10.1016/j.cropro.2017.05.003.
10. Zhao X, Cui H, Wang Y, Sun C, Cui B, Zeng Z. Development strategies and prospects of nano-based smart pesticide formulation. J Agric Food Chem. 2018;66:6504–12. DOI:10.1021/acs.jafc.7b02004.
11. Zhao GX, Wen T, Chen CL, Wang XK. Synthesis of graphene-based nanomaterials and their application in energy-related and environmental-related areas. Rsc Adv. 2012;2:9286–303. DOI:10.1039/c2ra20990j.

12. Kim WG, Han JK, Tcho IW, Park JY, Choi YK. Triboelectric nanogenerator for a repairable transistor with self-powered electro-thermal annealing. Nano Energy. 2020;76:105000. DOI:10.1016/j.nanoen.2020.105000.
13. Jiang LM, Yang Y, Chen Y, Zhou QF. Ultrasound-induced wireless energy harvesting: from materials strategies to functional applications. Nano Energy. 2020;77:105131. DOI:10.1016/j.nanoen.2020.105131.
14. Liu J, Zheng XP, Gu ZJ, Chen CY, Zhao YL. Bismuth sulfide nanorods as a precision nanomedicine for in vivo multimodal imaging-guided photothermal therapy of tumor. ACS Nano. 2016;12:486–7. DOI:10.1016/j.nano.2015.12.116.
15. Gopinath A, Miyazono E, Faraon A, Rothemund PWK. Engineering and mapping nanocavity emission via precision placement of DNA origami. Nature. 2016. DOI:10.1038/nature18287.
16. Kah M, Hofmann T. Nanopesticide research: Current trends and future priorities. Environ Int. 2014;63:224–35. DOI:10.1016/j.envint.2013.11.015.
17. Zhang HF, Wang D, Butler R, Campbell NL, Long J, Tan B, Duncalf DJ, Foster AJ, Hopkinson A, Taylor D, Angus D, Cooper AI, Rannard SP. Formation and enhanced biocidal activity of water-dispersable organic nanoparticles. Nat Nanotechnol. 2008;3:506–11. DOI:10.1038/nnano.2008.188.
18. Jia X, Sheng WB, Li W, Tong YB, Liu ZY, Zhou F. Adhesive polydopamine coated avermectin microcapsules for prolonging foliar pesticide retention. ACS Appl Mater Inter. 2014;6:19552–8. DOI:10.1021/am506458t.
19. Chariou PL, Steinmetz NF. Delivery of pesticides to plant parasitic nematodes using tobacco mild green mosaic virus as a nanocarrier. ACS Nano. 2017;11:4719–30. DOI:10.1021/acsnano.7b00823.
20. Li BX, Wang WC, Zhang XP, Zhang DX, Ren YP, Gao Y, Mu W, Liu F. Using coordination assembly as the microencapsulation strategy to promote the efficacy and environmental safety of pyraclostrobin, Adv Funct Mater 27 (2017). DOI:10.1002/adfm.201701841.
21. Liang Y, Fan C, Dong HQ, Zhang WB, Tang G, Yang JL, Jiang N, Cao YS. Preparation of MSNs-chitosan@prochloraz nanoparticles for reducing toxicity and improving release properties of prochloraz. ACS Sustain Chem Eng. 2018;6:10211–20. DOI:10.1021/acssuschemeng.8b01511.
22. Liang Y, Guo MC, Fan C, Dong HQ, Ding GL, Zhang WB, Tang G, Yang JL, Kong DD, Cao YS. Development of novel urease-responsive pendimethalin microcapsules using silica-IPTS-PEI As controlled release carrier materials. ACS Sustain Chem Eng. 2017;5:4802–10. DOI:10.1021/acssuschemeng.7b00208.
23. Jagadeesh RV, Murugesan K, Alshammari AS, Neumann H, Pohl MM, Radnik JR, Beller M. MOF-derived cobalt nanoparticles catalyze a general synthesis of amines, Science. (2017) 326. DOI:10.1126/science.aan6245.
24. Hurtley S, Yeston J, A MOF sets the stage to make amines, Science. 358 (2017) 316.312-318. DOI: 10.1126/science.358.6361.316-l.
25. Greathouse JA, Allendorf MD. The interaction of water with MOF-5 simulated by molecular dynamics. J Am Chem Soc. 2006;128:10678–9. DOI:10.1021/ja069972i.

26. Gould SL, Tranchemontagne D, Yaghi OM, Garcia-Garibay MA. Amphidynamic character of crystalline MOF-5: rotational dynamics of terephthalate phenylenes in a free-volume, sterically unhindered environment. J Am Chem Soc. 2008;130:3246–7. DOI:10.1021/ja077122c.
27. Yao C, Lykourinou V, Vetromile C, Hoang T, Ming LJ, Larsen RW, Ma SQ. How can proteins enter the interior of a MOF? Investigation of cytochrome translocation into a MOF consisting of mesoporous cages with microporous windows. J Am Chem Soc. 2012;134:13188–91. DOI:10.1021/ja305144x.
28. Khan S, Al-Shahry M, Jr W. Efficient photochemical water splitting by a chemically modified n-TiO2. Science. 2002;297:2243–5. DOI:10.1002/chin.200302016.
29. Alezi D, Belmabkhout Y, Suyetin M, Bhatt PM, Weselinski LJ, Solovyeva V, Adil K, Spanopoulos I, Trikalitis PN, Emwas AH. MOF crystal chemistry paving the way to gas storage needs: aluminum-based soc-MOF for CH_4, O_2, and CO_2 storage. J Am Chem Soc. 2015;137:13308–18. DOI:10.1021/jacs.5b07053.
30. Hartlieb KJ, Holcroft JM, Moghadam PZ, Vermeulen NA, Algaradah MM, Nassar MS, Botros YY, Snurr RQ, Stoddart JF. CD-MOF: a versatile separation medium. J Am Chem Soc. 2016;138:2292. DOI:10.1021/jacs.5b12860.
31. García-García P, Müller M, Corma A. MOF catalysis in relation to their homogeneous counterparts and conventional solid catalysts, Chem Sci 5 (2014). DOI:10.1039/C4SC00265B.
32. Vishnyakov A, Ravikovitch PI, Neimark AV, Bülow M. Nanopore structure and sorption properties of Cu – BTC metal organic framework. Nano Lett. 2003. DOI:10.1021/nl0341281.
33. Du M, Li LN, Li MX, Si R. Adsorption mechanism on metal organic frameworks of Cu-BTC, Fe-BTC and ZIF-8 for CO_2 capture investigated by X-ray absorption fine structure. Rsc Adv. 2016;6:62705–16. DOI:10.1039/C6RA07582G.
34. Nicolaou KC, Dolle RE, Papahatjis DP. Practical synthesis of oligosaccharides. Partial synthesis of avermectin B1a. J Am Chem Soc. 1984;106:4189–92. DOI:10.1021/ja00327a021.
35. He S, Zhang WD, Li DG, Li PL, Zhu YC, Ao MM, Li JQ, Cao YS. Preparation and characterization of double-shelled avermectin microcapsules based on copolymer matrix of silica–glutaraldehyde–chitosan. J Mater Chem B. 2013;1:1270–8. DOI:10.1039/c2tb00234e.
36. Schroeder M. Trapping strategy for *Monochamus sutor* and *Monochamus galloprovincialis*: potential vectors of the pine wood nematode in Scandinavia. Agr Forest Entomol. 2019;21:372–8. DOI:10.1111/afe.12339.
37. Eddaoudi M, Kim J, Rosi N, Vodak D, Wachter J, O'Keeffe M, Yaghi OM. Systematic design of pore size and functionality in isoreticular MOFs and their application in methane storage. Science. 2002;295:469–72. DOI:10.1126/science.1067208.
38. Li YP, Li XY, Guan QX, Zhang CJ, Xu T, Dong YJ, Bai XY, Zhang WP. Strategy for chemotherapeutic delivery using a nanosized porous metal-organic framework with a central composite design. Int J Nanomed Volume. 2017;12:1465–74. DOI:10.2147/IJN.S119115.
39. Su CY, Ji YC, Liu SS, Gao SK, Cao SH, Xu XY, Zhou CG, Liu YX. Fluorescence-labeled abamectin nanopesticide for comprehensive control of pinewood nematode and *Monochamus alternatus* Hope.

ACS Sustain Chem Eng. 2020;8:16555–64. DOI:10.1021/acssuschemeng.0c05771.

40. Li YX, Zhou MS, Pang YX, Qiu XQ. Lignin-based microsphere: preparation and performance on encapsulating the pesticide avermectin. ACS Sustain Chem Eng. 2017;5:3321–8. DOI:10.1021/acssuschemeng.6b03180.
41. Guo MC, Zhang WB, Ding GL, Guo D, Zhu JL, Wang BT, Punyapitak D, Cao YS. Preparation and characterization of enzyme-responsive emamectin benzoate microcapsules based on a copolymer matrix of silica–epichlorohydrin–carboxymethylcellulose. Rsc Adv. 2015;5:93170–9. DOI:10.1039/C5RA17901G.
42. Su CY, Liu SS, Cao SH, Yin SY, Zhou CG, Gao SK, Jia CY, Ji YC, Liu YX. Self-assembled bovine serum albumin nanoparticles as pesticide delivery vectors for controlling trunk-boring pests, J Nanobiotechnol. 18 (2020). DOI:10.1186/s12951-020-00725-z.
43. Albersschoenberg G, Arison BH, Chabala JC, Douglas AW, Eskola P, Fisher MH, Lusi A, Mrozik H, Smith JL, Tolman RL. Avermectins. Structure determination. J Am Chem Soc. 1981;103:4216–21. DOI:10.1021/ja00404a040.
44. Manuel FP. Controlled release systems to prevent the agro-environmental pollution derived from pesticide use. J Environ Sci Heal B. 2007;42:857–62. DOI:10.1080/03601230701555138.

Figures

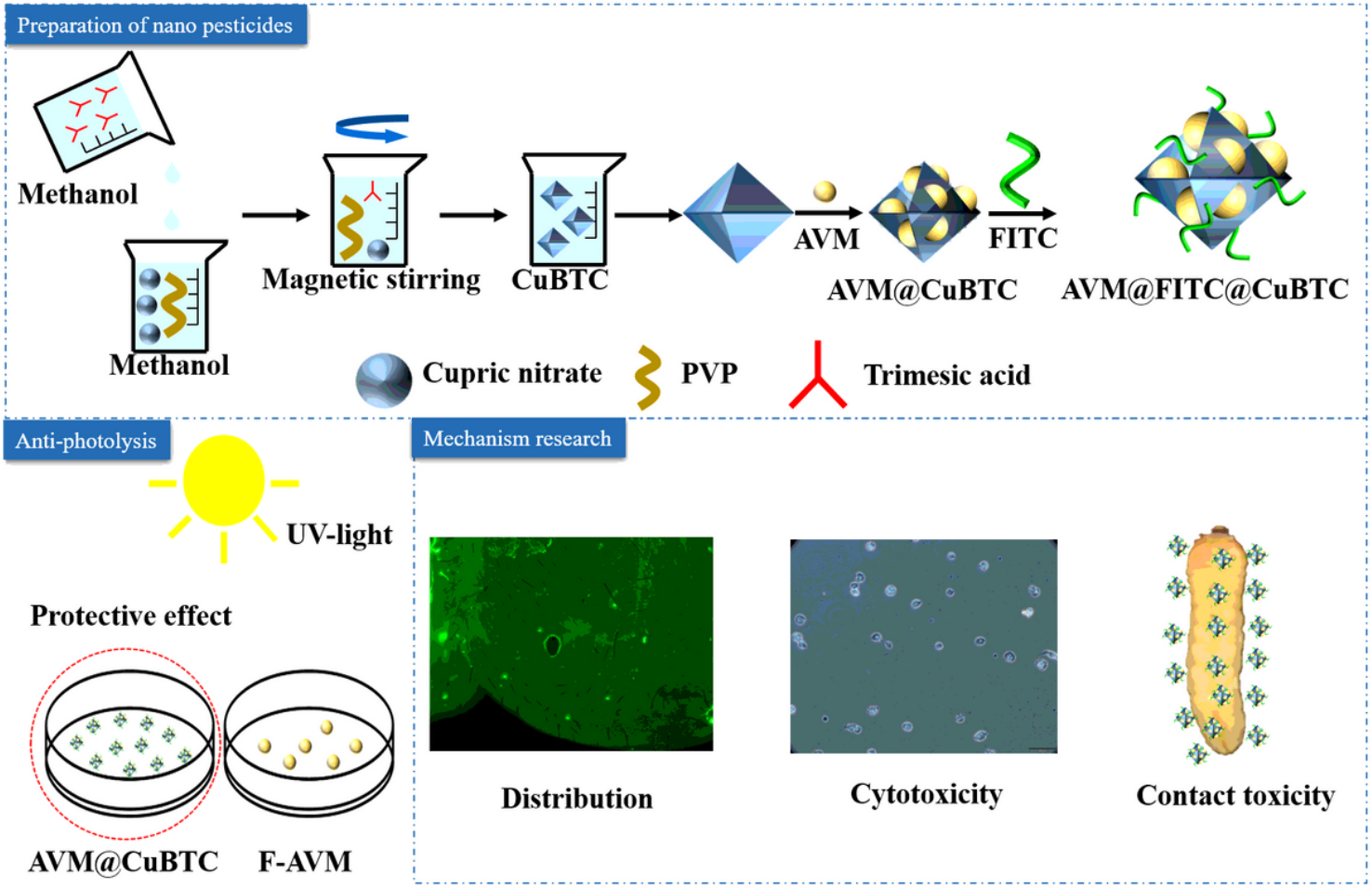

Figure 1

Schematic illustration of the AVM@CuBTC, it could adsorb the hydrophobic drug AVM and was labeled with fluorescein isothiocyanate for pest control, for protecting AVM from photolysis, for exploring the distribution and cytotoxicity of AVM@CuBTC, for researching the contact toxicity.

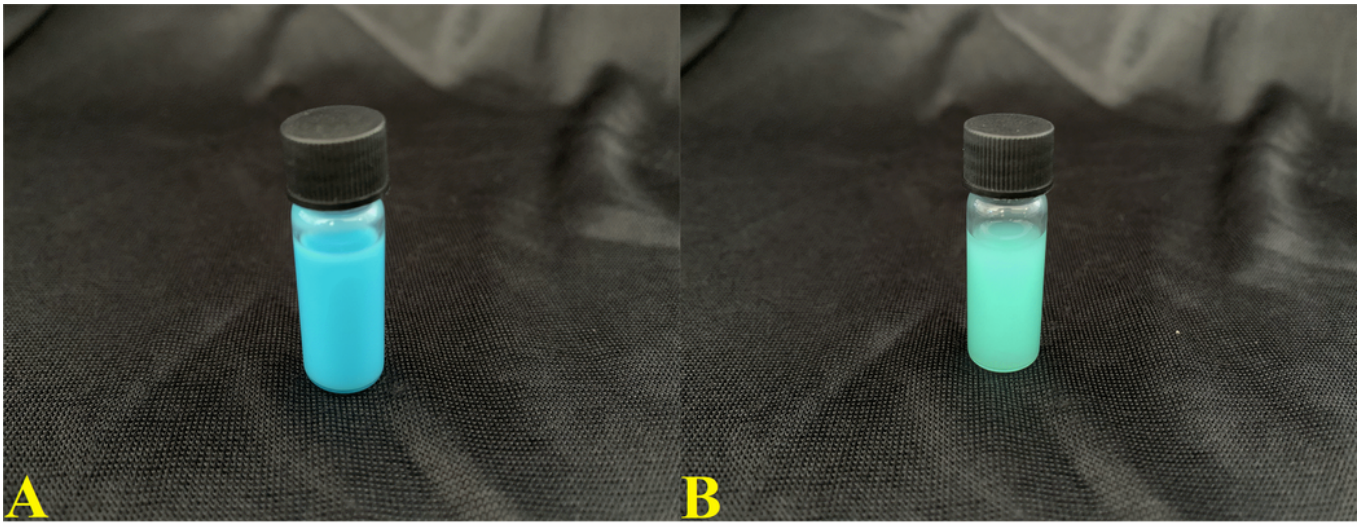

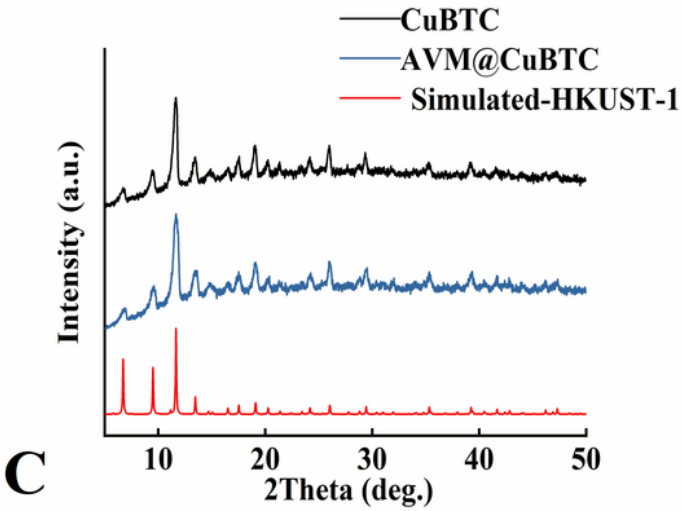

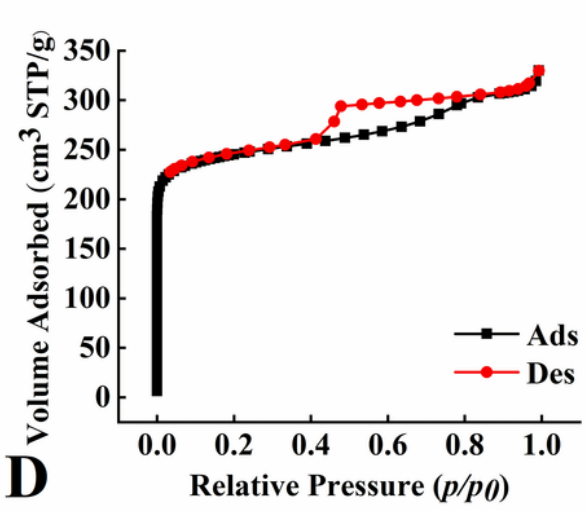

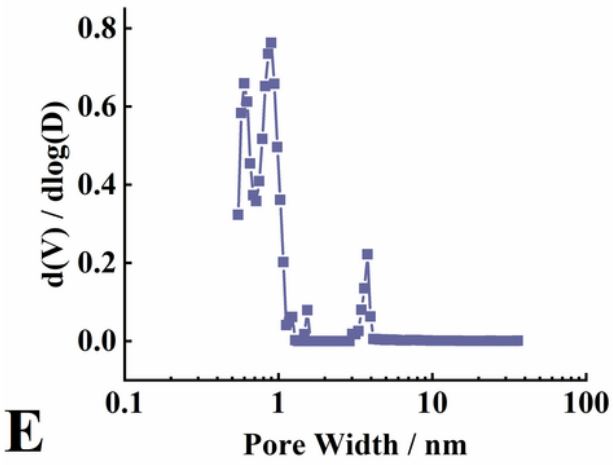

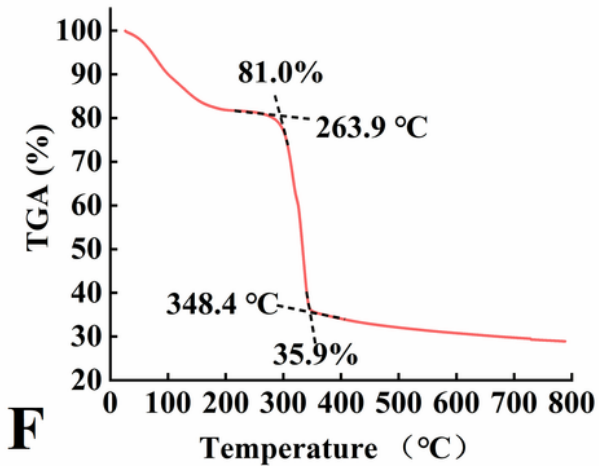

Figure 2

The AVM@CuBTC (A) and AVM@FITC@CuBTC (B) aqueous solution, and the XRD (C), adsorption curve (D), pore width (E), and TGA (F) of CuBTC.

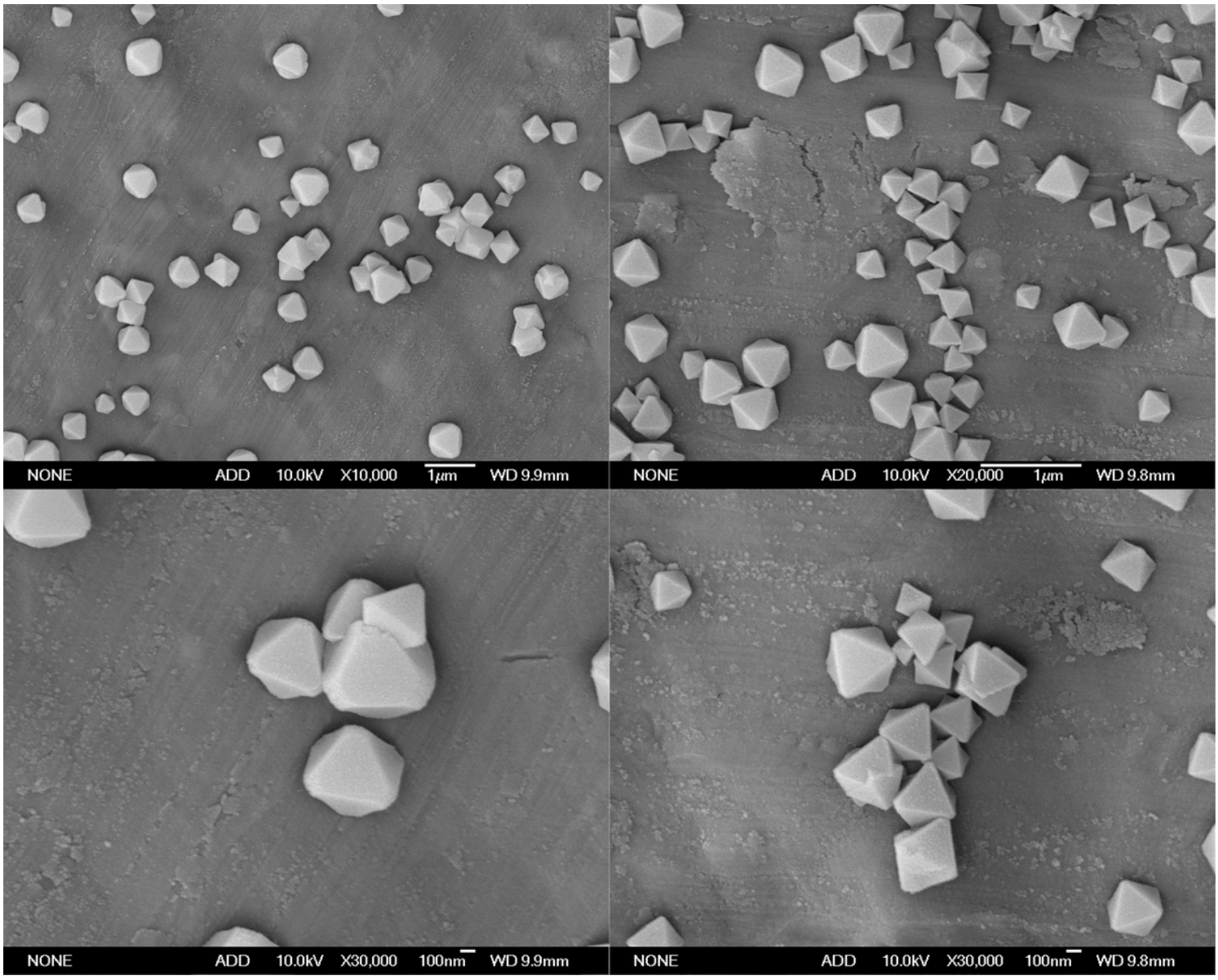

Figure 3

The SEM images of AVM@CuBTC.

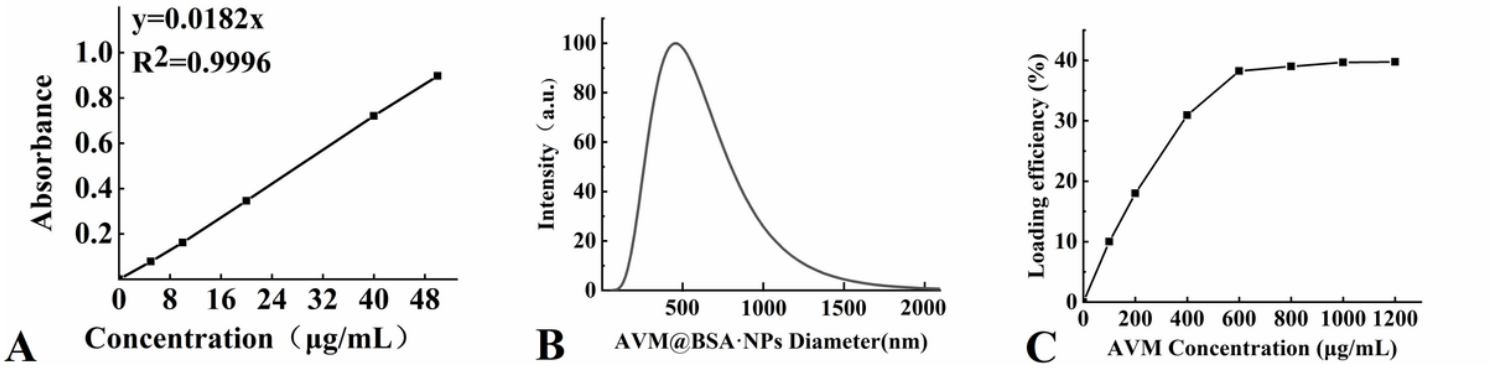

Figure 4

The standard curve of AVM in methanol (A), particle size distribution (B), loading efficiency of AVM@CuBTC with different concentration of AVM (C).

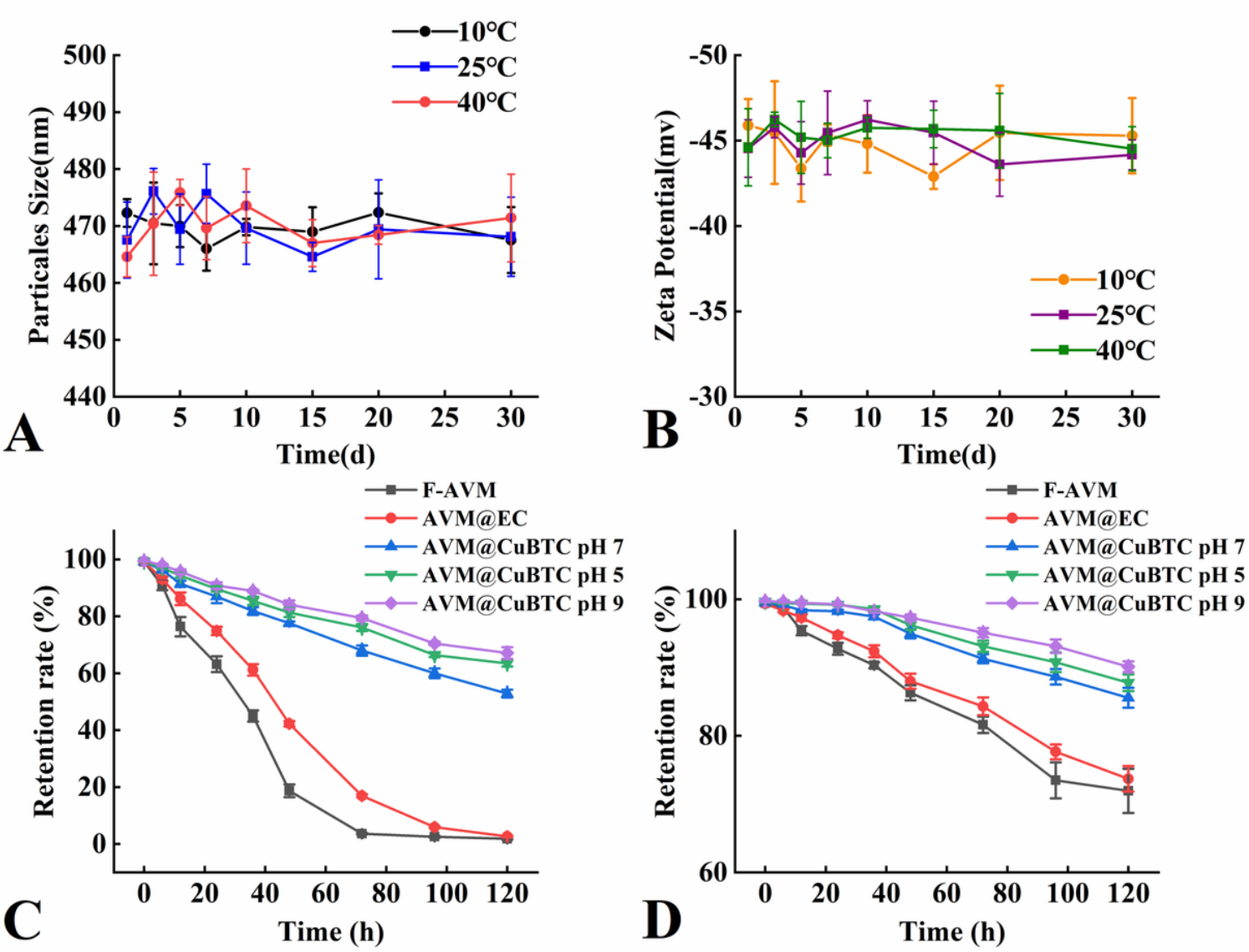

Figure 5

The changes of particle size (A) and Zeta potential (B) in 45 d, the retention rate of AVM in F-AVM, AVM@EC, AVM@CuBTC, AVM@CuBTC pH 5.0, AVM@CuBTC pH 9.0 after being exposed to ultraviolet light (C) and dark condition(D).

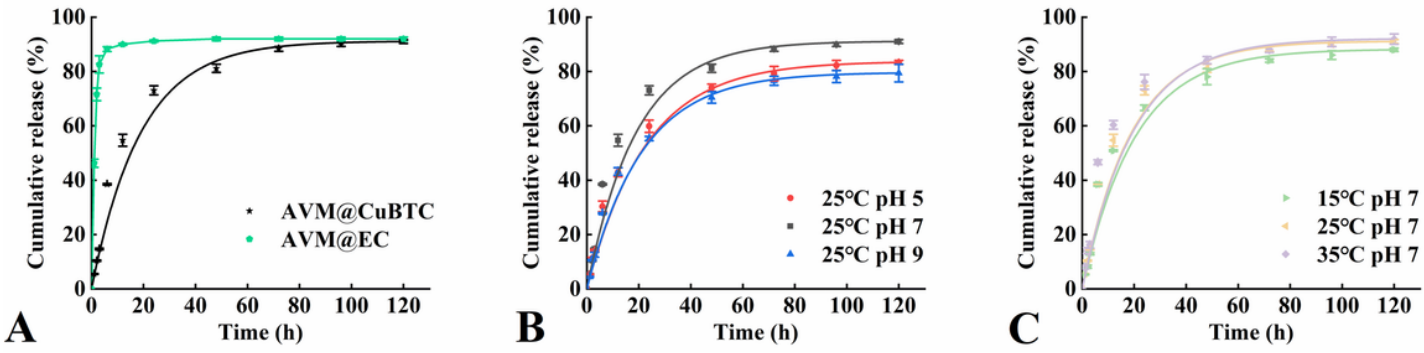

Figure 6

The release curves of AVM@CuBTC and AVM@EC (A), at different temperatures (B), and pH vlaves (C).

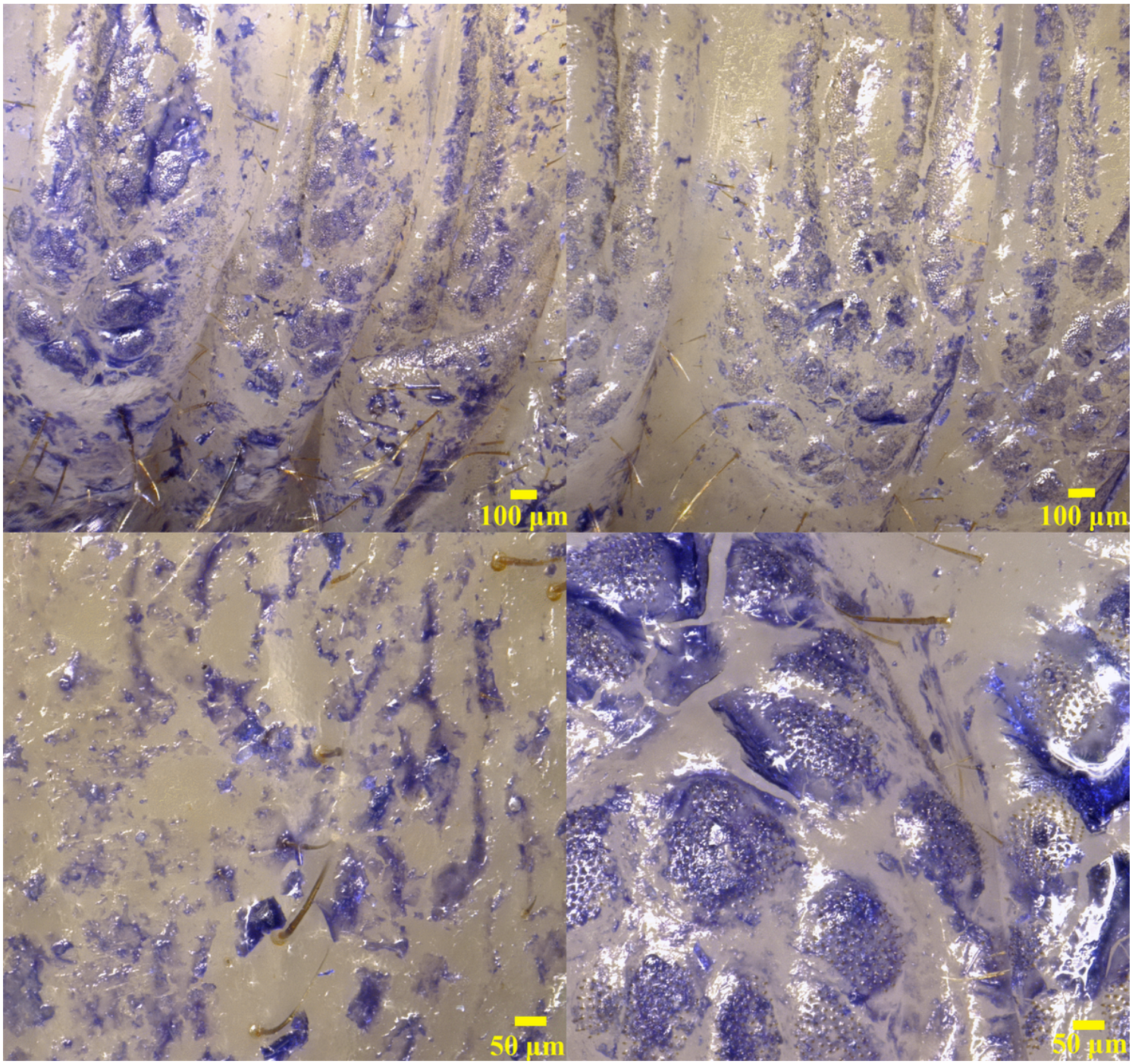

Figure 7

The distribution of AVM@CuBTC observed by ultra-depth-of-field microscope.

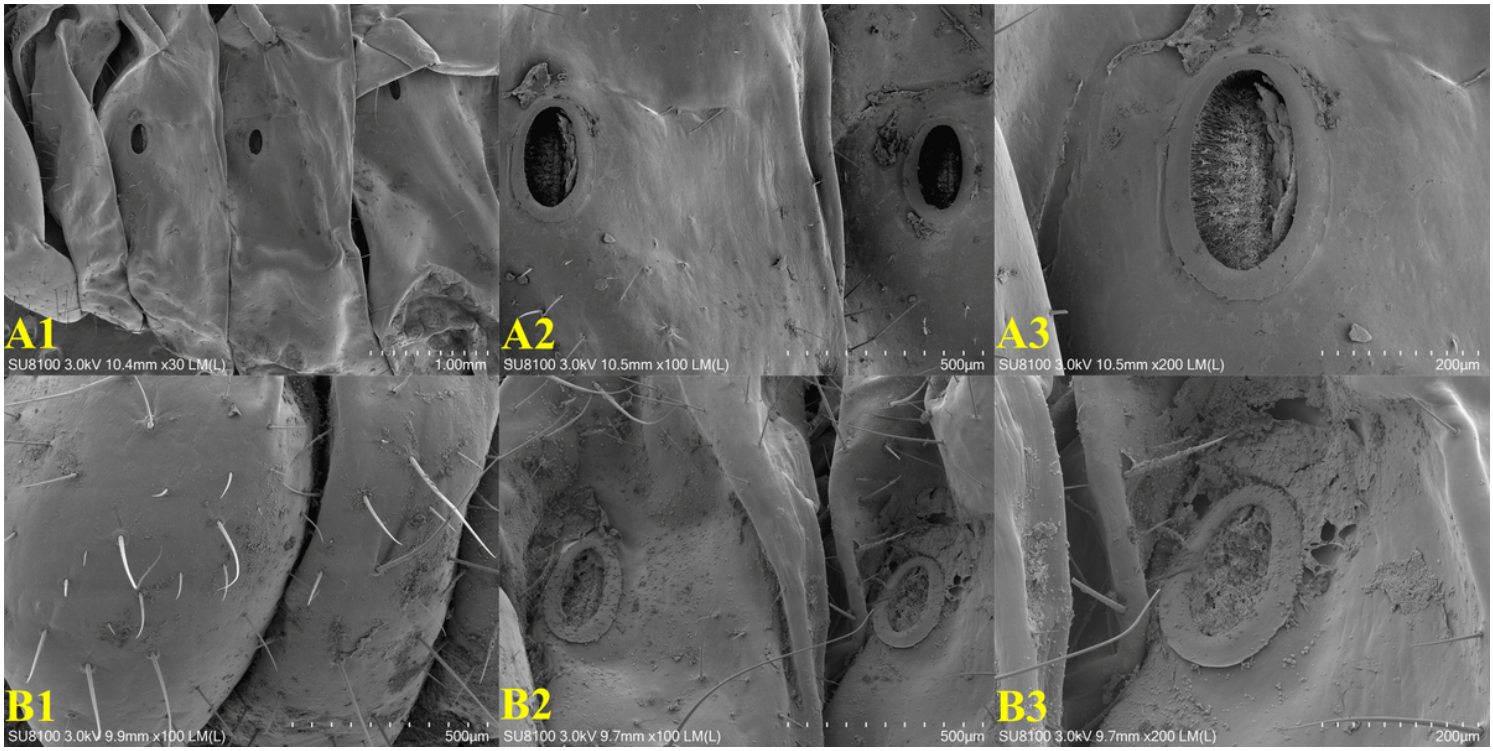

Figure 8

The SEM images of larval epidermis (A1-A3) and the distribution of AVM@CuBTC(B1-B3).

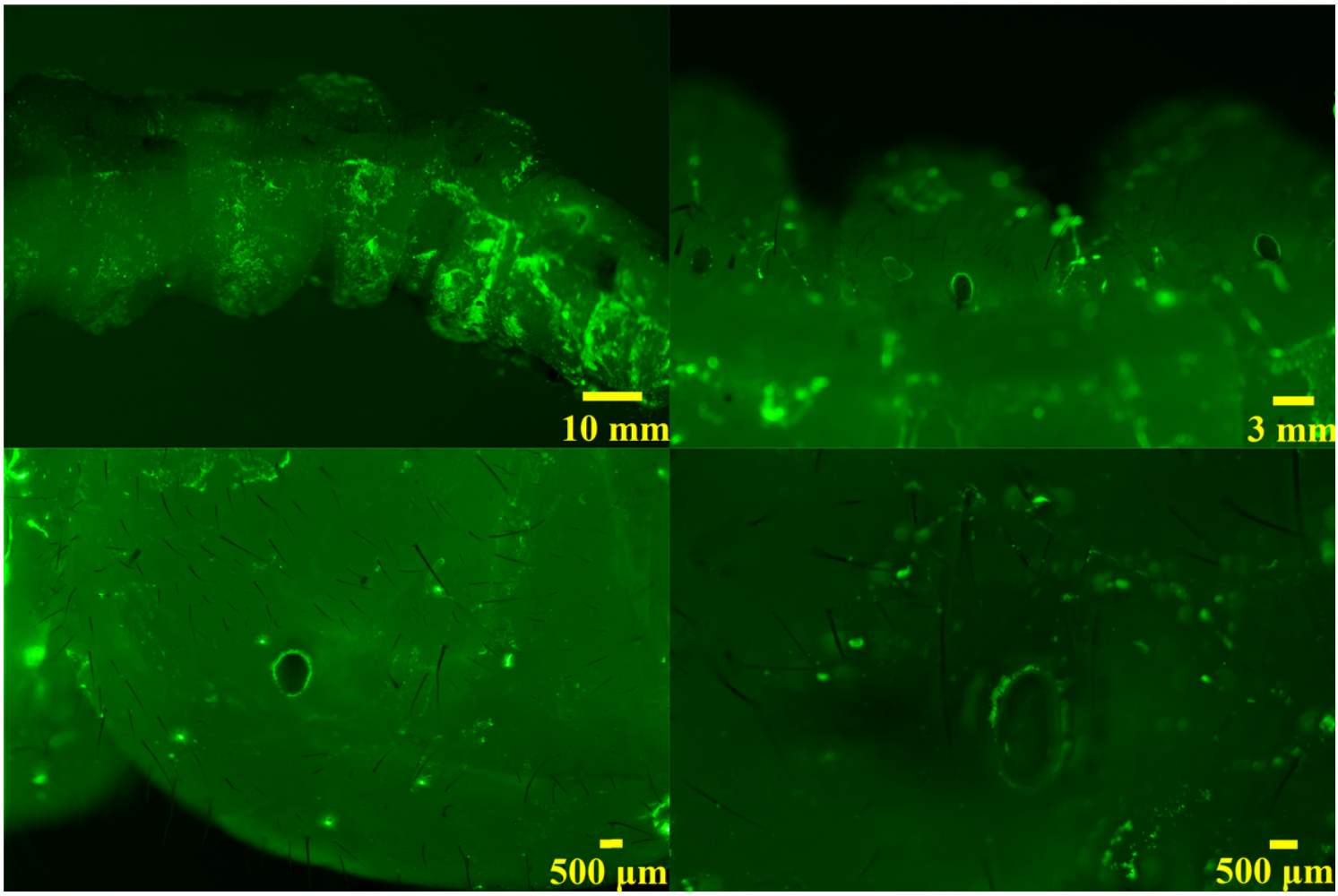

Figure 9

The fluorescence distribution image of AVM@FITC@CuBTC.

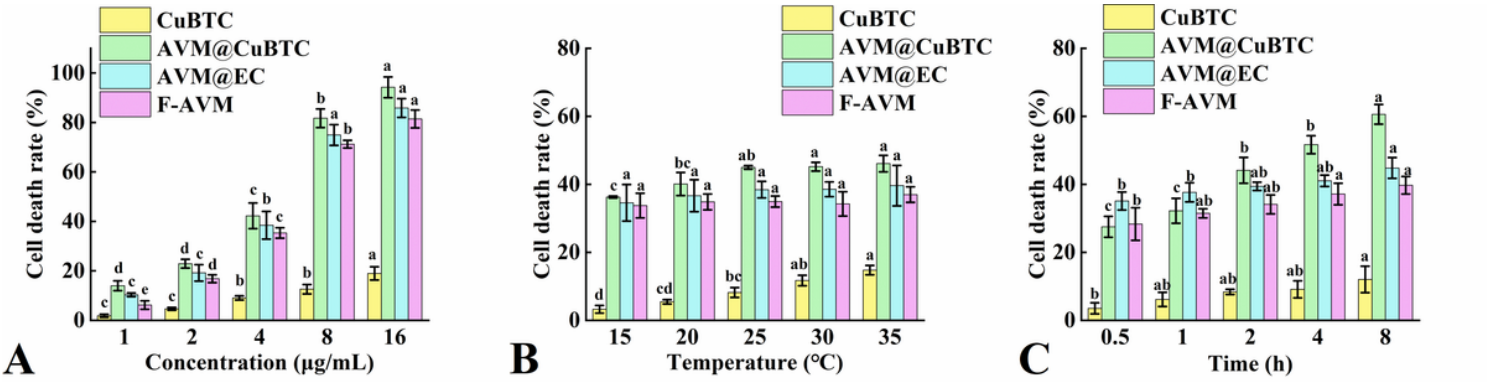

Figure 10

The cytotoxicity of CuBTC, AVM@CuBTC, AVM@EC, and F-AVM at different concentrations (A), temperatures (B, times (C).

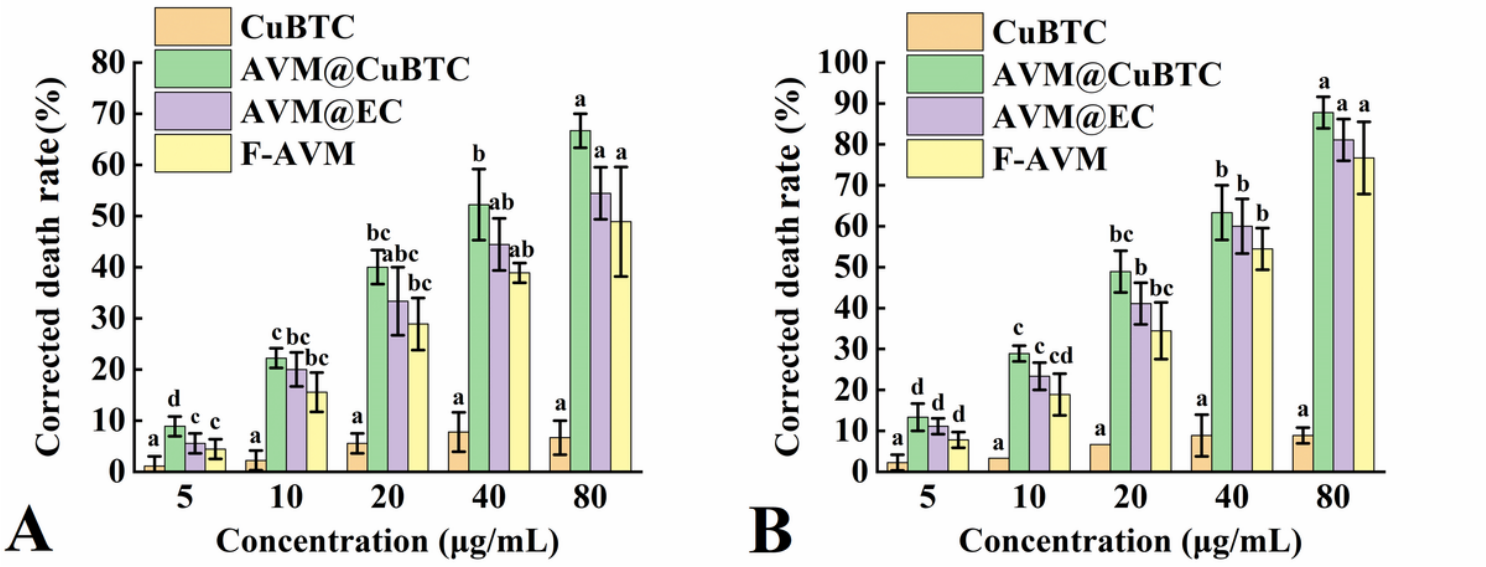

Figure 11

The contact toxicity of CuBTC, AVM@CuBTC, AVM@EC, and F-AVM at 24 h (A), 48 h(B).